ORCHIDEE-CROP (v0), a new process based Agro-Land Surface Model: model description and evaluation over Europe

Xiuchen Wu[1,2*], Nicolas Vuichard[1*], Philippe Ciais[1], Nicolas Viovy[1], Nathalie de Noblet-Ducoudré[1], Xuhui Wang[3], Vincenzo Magliulo[4], Martin Wattenbach[5], Luca Vitale[4], Paul Di Tommasi[4], Eddy J Moors[6], Wilma Jans[6], Jan Elbers[6], Eric Ceschia[7], Tiphaine Tallec[7], Christian Bernhofer[8], Thomas Grünwald[8], Christine Moureaux[9], Tanguy Manise[9], Anne Ligne[9], Pierre Cellier[10], Benjamin Loubet[10], Eric Larmanou[10], Dominique Ripoche[11]

1. CEA-CNRS-UVSQ, UMR8212-Laboratoire des Sciences du Climat et de l'Environnement (LSCE), Orme des Merisiers, 91191, Gif-Sur-Yvette, France

2. College of Resources Science and Technology, Beijing Normal University, Beijing 100875, China

3. Sino-French Institute for Earth System Science, College of Urban and Environmental Sciences, Peking University, Beijing 100871, China

4. Istituto per i Sistemi Agricoli e Forestali del Mediterraneo, CNR, Via C. Patacca 85, 80056 Ercolano (Napoli), Italy

5. Helmholtz Centre Potsdam GFZ German Research Centre For Geosciences, Deutsches GeoForschungsZentrum GFZ, Telegrafenberg, 14473, Potsdam, Germany

6. Wageningen UR, Alterra, Earth System Science and Climate Change Group, P.O. Box 47, 6700 AA Wageningen, The Netherlands

7. CESBIO, UMR 5126 - CNES-CNRS-UPS-IRD- 18 avenue Edouard Belin 31401 Toulouse cedex 9, France

8. Technische Universität Dresden, Institute of Hydrology and Meteorology, Pienner Str. 23, D-01737 Tharandt, Germany

9. Université de Liège – Gembloux Agro-Bio Tech, Crops Management Unit, 5030 Gembloux, Belgium

10. INRA, UMR INRA-AgroParisTech ECOSYS (Ecologie fonctionnelle et écotoxicologie des agro- écosystèmes), 78850 Thiverval-Grignon, France

11. INRA, US1116 AgroClim, Avignon, France

*Correspondence:

Xiuchen Wu: xiuchen.wu@bnu.edu.cn; Tel: 0086-10-58807052; Fax: 0086-10-58807656;

Nicolas Vuichard: nicolas.vuichard@lsce.ipsl.fr; Tel: 0033-1-69084226; Fax: 0033-1-69083073;

Abstract:

The response of crops to changing climate and atmospheric CO_2 concentration ($[CO_2]$) could have large effects on food production, and impact carbon, water, and energy fluxes, causing feedbacks to the climate. To simulate the response of temperate crops to changing climate and $[CO_2]$, which accounts for the specific phenology of crops mediated by management practice, we describe here the development of a process-oriented terrestrial biogeochemical model named ORCHIDEE-CROP (v0), which integrates a generic crop phenology and harvest module, and a very simple parameterization of nitrogen fertilization, into the land surface model (LSM) ORCHIDEEv196, in order to simulate biophysical and biochemical interactions in croplands, as well as plant productivity and harvested yield. The model is applicable for a range of temperate crops, but is tested here using maize and winter wheat, with the phenological parameterizations of two European varieties originating from the STICS agronomical model. We evaluate the ORCHIDEE-CROP (v0) model against eddy covariance and biometric measurements at seven winter wheat and maize sites in Europe. The specific ecosystem variables used in the evaluation are CO_2 fluxes (net ecosystem exchange (NEE)), latent heat, and sensible heat fluxes. Additional measurements of leaf area index (LAI), aboveground biomass and yield are used as well. Evaluation results revealed that ORCHIDEE-CROP (v0) reproduced the observed timing of crop development stages and the amplitude of the LAI changes. This is in contrast to ORCHIDEEv196 where, by default, crops have the same phenology as grass.

A halving of the root mean square error for LAI from 2.38 ±0.77 m^2 m^{-2} to 1.08 ±0.34 m^2 m^{-2} was obtained when ORCHIDEEv196 and ORCHIDEE-CROP (v0) were compared across the seven study sites. Improved crop phenology and carbon allocation led to a good match between modelled and observed aboveground biomass (with a normalized root mean squared error (NRMSE) of 11.0%–54.2%), crop yield, daily carbon and energy fluxes (with a NRMSE of ~ 9.0%–20.1% and ~ 9.4%–22.3% for NEE), and sensible and latent heat fluxes. The simulated yields for winter wheat and maize from ORCHIDEE-CROP (v0) showed a good match with the simulated results from STICS for three sites with available crop yield observations, where the average NRMSE was ~8.8%. The model data misfit for energy fluxes were within the uncertainties of the measurements, which themselves showed an incomplete energy balance closure within the range 80.6%–86.3%. The remaining discrepancies between the modeled and observed LAI and other variables at specific sites were partly attributable to unrealistic representations of management events by the model. ORCHIDEE-CROP (v0) has the ability to capture the spatial gradients of carbon and energy-related variables, such as gross primary productivity, NEE, and sensible and latent heat fluxes across the sites in Europe, which is an important requirement for future spatially explicit simulations. Further improvement of the model, with an explicit parameterization of nutritional dynamics and management, is expected to improve its predictive ability to simulate croplands in an Earth System Model.

Keywords: Crop model, ORCHIDEE-CROP, STICS, Crop yield, Energy balance, Net

Introduction

Croplands cover about 12% of the world land surface (Ramankutty and Foley, 1998), with temporal and spatial variations being subject to population increase, changes in diet, market prices, and other socio-economic factors (IPCC, 2014; Ramankutty et al., 2002; Vuichard et al., 2008). The response of croplands to climate change is expected to have significant, but uncertain, consequences for 1) global food production and 2) land surface water, carbon, and energy fluxes, which affect food security as well as regional climate and water resources (Bonan, 2008, 2001; Loarie et al., 2011; Rosenzweig et al., 2014).

Along with improving understanding of crop physiology to increase production and yield quality, research has focused on investigating the climate impacts on crop functioning by combining historical observations with statistical models (Lobell and Field, 2007; Lobell et al., 2011; Rosenzweig and Parry, 1994) or by running crop models from site to global scales. Impact studies have always pointed to the significant effect of climate on crop yield variability (Lobell and Field, 2007; Parry et al., 2005; Rosenzweig et al., 2013). However, discrepancies in the response to climate change between different crop models have highlighted the uncertainties that are related to model structure, parameterization, and external drivers (Asseng et al., 2013; Müller, 2011; Rosenzweig et al., 2013).

There is an increasing need to improve understanding of the environmental and climate consequences of changes in cropland area and in management practices, via

modification of biophysical and biogeochemical land-atmosphere fluxes (Foley et al., 2011; Lobell et al., 2006; Osborne et al., 2009; Tubiello et al., 2007). Many lines of evidence show that changes of cropland plant properties can strongly modify the biophysical characteristics (albedo, roughness, turbulent fluxes) of the land surface, which affect local and regional climates (Davin et al., 2014; Foley et al., 2011; Georgescu et al., 2009; Loarie et al., 2011; Osborne et al., 2009).

Investigation of cropland-climate interactions has led to new model developments that improve Land Surface Models (LSMs) so that they give a more realistic representation of crop processes (Bondeau et al., 2007; Gervois et al., 2004; Kucharik, 2003). The aim is to simulate the spatial distribution and variability of crop production and its water, energy, and carbon fluxes, all of which affect climate. These efforts have improved the seasonal dynamics of modeled foliar and biomass developments (Bondeau et al., 2007; Gervois et al., 2008; Gervois et al., 2004; Kucharik, 2003; Valade et al., 2014; Van den Hoof et al., 2011) and long-term soil carbon changes (Ciais et al., 2011). Despite progress, these "Agro-LSM" models have some limitations, such as 1) static or crop/region specific parameterizations (Berg et al., 2011; Kucharik, 2003); 2) idealized representation of different crop types and cultivation practices (Bondeau et al., 2007); and 3) incomplete coupling between crop growth parameterizations and LSM processes (de Noblet-Ducoudré et al., 2004; Gervois et al., 2004; Valade et al., 2014).

In this study, we integrate a generic crop phenology and allocation module from the STICS agronomical model, which has been extensively validated and can simulate different crops (e.g., wheat, maize, soybean, bananas) (Brisson et al., 1998; Brisson et

al., 2002) into the carbon-water-energy LSM ORCHIDEE model (Krinner et al., 2005), resulting in a new Agro-Land Surface Model, ORCHIDEE-CROP (at version v0, hereafter referred to as ORCHIDEE-CROP, https://forge.ipsl.jussieu.fr/orchidee/wiki/DevelopmentActivities). ORCHIDEE-CROP has two applications: offline and online. Offline applications (presented here) improve understanding of the mechanisms controlling yield, given climate and management forcing. Online simulations require the crop model to be coupled with an atmospheric model (GCM) when studying crop vegetation feedbacks on climate. Several crop models have been developed for offline applications and impact studies, but very few of these models can be coupled with GCMs, e.g. because they do not represent albedo, roughness, and sensible and latent heat fluxes on the typical time step of ≈ 30 min, which are required to couple with a GCM.

Our efforts have focused on improving the representation of phenology, the simulation of biophysical and biogeochemical fluxes, and on biomass and grain yields. ORCHIDEE-CROP can solve the incomplete coupling problems in the existing ORCHIDEE-STICS model (Gervois et al., 2004).

We first describe the structure of ORCHIDEE-CROP (section 2) and evaluate the new model for phenology, CO_2, and energy fluxes over winter wheat and maize sites across a large climate gradient in Europe using observations of biophysical and carbon variables (LAI, biomass, latent (LE) and sensible heat (H) fluxes, and net ecosystem exchange, NEE) from seven eddy covariance sites (section 3). Finally, we discuss the general performance of ORCHIDEE-CROP, its limitations and the future research that

152 is needed (section 4).

153 **2. Materials and methods**

154 **2.1 Model description**

155 Two key processes of crop plants were introduced into a module integrated in
156 ORCHIDEEv196 (version Tag196, http://forge.ipsl.jussieu.fr/orchidee/wiki/Tags/196,
157 called ORCHIDEE hereafter). This module simulates crop phenology and the specific
158 carbon allocation to grain prior to harvest (Fig. 1). This crop module is used to calculate
159 1) the seasonal dynamics of LAI, a key variable that impacts surface biophysical
160 properties (albedo, roughness) and water, energy and carbon fluxes, and 2) the timing
161 and amount of grain filling that determines yield.
162 In ORCHIDEE, the vegetation is divided into 13 plant function types (PFTs),
163 including bare soil, 10 natural PFTs (e.g., evergreen and deciduous trees, C3, and C4
164 grass) and two crop PFTs (C3 and C4 crops) that are assumed to have the same
165 phenology as natural grasslands, but with higher carboxylation rates (Krinner et al.,
166 2005). More vegetation types can be simulated using a new PFT external definition
167 module (http://labex.ipsl.fr/orchidee/index.php/about-orchidee). Several PFTs can
168 coexist within the same grid cell (also referred to as mosaic vegetation) which can
169 have any size, generally given by the spatial resolution of climate forcing data. All
170 PFTs that co-exist within a grid cell share the same climate forcing but different
171 carbon, energy and water dynamics, due to their specific parameterizations. The sum
172 of fluxes from the different PFT tiles is averaged before being entered into the

atmospheric model, in order to avoid coupled simulations.

2.1.1 Crop development stages and phenology in ORCHIDEE-CROP

A thermal index (degree-day) adjusted for photoperiodic and vernalization effects according to crop types, controls the developments of temperate crops, such as winter wheat and maize considered here. Seven development stages are sequentially simulated for crop growth and grain filling in the crop module, which is the same as the processes in STICS (Fig. 1 in Brisson et al., 1998). The timing and duration of each stage is calculated based on development units, which describe the physiological requirements of crops. These development units are calculated, as in STICS, as growing degree days weighted by limiting functions to account for photoperiodism (e.g., winter wheat and soybean) and vernalization (e.g., winter wheat). Vernalization requirement is defined as a given number of vernalizing days (JVC) since the crop germination, and requires a minimum of 7 vernalizing days. The vernalizing value of a given day (JVI) is a function of air temperature. The vernalization status (RFVI) of the vernalization sensitive crop increases gradually to one when the vernalization requirement is met (Supplementary Eqn. 1). The photoperiodic slowing effect, RFPI, is determined by two photoperiod thresholds, PHOBASE and PHOSAT, for photoperiodic crops. In the case of short-day crops, the PHOBASE is higher than PHOSAT, whereas in the case of long-day crops, the PHOBASE is lower than PHOSAT. The current photoperiod PHOI is calculated on the basis of calendar days and latitude (Sellers, 1965) (Supplementary Eqn. 2). Transition between stages occurs when the threshold values of development units are

reached, which are specific to different crops or cultivars, but also depend upon management intensity and local climate. Using generic terms for the various plant development stages makes it possible to simulate different kinds of crops if crop-specific parameter values are provided (Bassu et al., 2014; Brisson et al., 2002; Valade et al., 2014).

Crop emergence occurs during the sowing-emergence stage, and is divided into seed germination and epicotyl extension. Germination occurs when the sum of degree-days, using the soil temperature (TSOL) at the sowing depth (PROFSEM), reaches a given threshold (STPLTGER) and is dependent on soil dryness (Supplementary Eqn. 3). The growth rate of the epicotyl is assumed to be a logistic function that depends on soil temperature and water status at the sowing depth (Supplementary Eqn. 4). Crop emergence occurs when the epicotyl elongates and is dependent on planting depth (PROFSEM). The actual density of emerged plants is calculated from the initial sowing density, a fixed parameter, which takes into account some lack of germination and the death of a fraction of young plants due to unsuitable soil moisture (humectation or drought) and/or to thermal time deficit (Brisson et al., 2008). During this stage, extremely cold temperatures can reduce the seedling density through its effects on both vernalization and thermal limits for cold-sensitive crops (e.g., winter wheat). From emergence to physiological maturity, the temporal evolution of LAI is calculated in the crop module as the net balance between leaf growth and senescence. The daily growth rate of LAI (DELTAI) is calculated based on a logistic function of development units ($DELTAI_{dev}$, related to different development stages) multiplied by an effective crop

temperature, an effective plant density, which takes the inter-plant competition into account, and stress functions ($DELTAI_{stress}$) related to water and nitrogen limitations (Supplementary Eqn. 5) (Brisson et al., 1998). The leaf senescence depends upon the evolution of temperature and leaf lifespan as a function of leaf development and stresses (e.g., water stress). Consequently, leaf senescence is updated each day (Brisson et al., 2008). Extremely hot and/or cold temperatures from crop emergence to maturity can affect leaf dynamics through its effects on both the daily leaf growth increment and leaf senescence of crops, and thus significantly affects photosynthesis and carbon allocations.

2.1.2 Photosynthesis, carbon allocation and yield

In ORCHIDEE-CROP, photosynthesis is calculated using ORCHIDEE (Krinner et al., 2005), which is based on the Farquhar leaf photosynthesis model for C3 crops (Farquhar et al., 1980) and on the model developed by Collatz *et al.* for C4 crops (Collatz et al., 1992). In both cases, photosynthetic rate is the minimum of the Rubisco-limited rate for CO_2 assimilation and the electron transport-limited rate for CO_2 assimilation, whose maximal values are the model parameters V_{cmax} and V_{jmax}, respectively. These two parameters can be calibrated using, for instance, the leaf-level measurements for different kinds of crops and varieties.

In ORCHIDEE, the carbon allocation model common to all PFTs is adapted from Friedlingstein *et al.*(Friedlingstein et al., 1999) and accounts for eight biomass compartments (leaves, roots, fruits/harvested organs, reserves, aboveground sapwood,

belowground sapwood, aboveground heartwood, and belowground heartwood) for trees, and considers five carbon pools for grass and crop PFTs (leaves, roots, fruits/harvested organs, reserves, and aboveground sapwood). The fractions of newly formed assimilates or reserves allocated to these pools are parameterized as a function of soil water content, temperature, light, and soil nitrogen availability.

In ORCHIDEE-CROP, we modified the carbon allocation scheme of the two crop PFTs to reconcile the calculations for leaf and root biomass and grain yield (fruits/harvested organs), which are driven by the phenology and LAI development parameterizations described in section 2.1.1. Specifically, the daily increment of leaf biomass for crops, Δ_{leaf_m}, is calculated by dividing the daily change in LAI, Δ_{LAI}, by specific leaf area (*sla*), which is weighted by the water and nitrogen stress factors (Brisson et al., 2008) as given by

$$\Delta_{leaf\_m} = \Delta_{LAI} / sla \quad (1)$$

The daily increment for root biomass is determined by the daily total biomass increment and a daily dynamic belowground-to-total biomass partition coefficient, which depends on root development through a normalized root development unit. After the start of the grain filling stage, the dry matter accumulation in grains is calculated using a "*harvest index*" function that determines the daily fraction of the increment for the total biomass allocated to grain filling. This "*harvest index*" function increases linearly with time from the start of grain filling to the physiological maturity of the crop (when crop is harvested), and is restricted by an upper limit. The effects of extreme temperature on the grain filling process are described in Supplementary Eq. 6 (Brisson et al., 2008).

The remaining daily net primary production (NPP), once allocation to leaf, root, and grain biomass is performed (the latter occurring only after the start of the grain filling phase), is allocated to the stem compartment to conserve mass. This “residual” stem compartment denotes both the actual stem biomass and additional reserves. At harvest, a small part of the carbon (with the same amount allotted to planted seeds) is moved from harvested organs to the reserves pool. This mimics the amount of carbon that seeds need for the next crop season.

In ORCHIDEE-CROP, the carbon allocation priority to different compartments was changed so that it was consistent with the growth development phases derived from STICS. In the vegetative stages, the leaf and root have the highest priority. If the NPP supply cannot satisfy the leaf and root biomass demand, no carbon is allocated to stems and the required amount of carbon demanded for leaf and root growth is removed from the reserves. If the extreme case occurs, in which the reserves are not sufficient, the amount of NPP allocated to leaf and root is reduced in proportion to the shoot/root ratio (no carbon being allocated to the stem). However, in such extreme cases, the consistency between LAI and leaf biomass is lost. Conversely, during the reproductive stage, carbon allocation is prioritized to grain filling and leaf biomass, followed by stem and root allocation of the remaining NPP. If the NPP available after satisfying the grain demand is not sufficient to support the allocation to the leaf, then carbon is remobilized from stem and root according to a fixed shoot/root ratio.

2.1.3 Soil moisture limitation effect on plant growth

Water limitation for crop development and biomass production is accounted for through a water stress index calculated from ORCHIDEE, and ranges from 0 to 1. It allows for reduced leaf growth and accelerated leaf senescence rates. The root water uptake function in ORCHIDEE is based on the assumption that the vertical root density distribution exponentially decreases with depth (Krinner et al., 2005) and that water uptake is a function of root zone extractible water weighted by the root profile. Relative water content in the root zone is an index defined by the difference between actual water content and the wilting point, divided by the difference between field capacity and the wilting point. This index always varies between 0 and 1. Below a fixed relative root zone water content threshold of 0.5, the ORCHIDEE stress index value decreases from 1 (no stress) to zero (wilting point). This stress index is used as a multiplier for both V_{cmax} and stomatal conductance, and leads to a decrease in gross primary productivity and transpiration.

Two different soil hydrological schemes, namely a two layer soil scheme, referred to as 2LAY, and an 11 layer soil diffusion scheme, referred to as 11LAY ((Guimberteau et al., 2014) were used in this study to calculate soil moisture and all dependent ecosystem state variables. In ORCHIDEE-CROP (V0), soil hydrology is simulated for three separate soil tiles in each grid cell. These three tiles are covered by bare soil, short vegetation (including crops), and by forest vegetation. Here, for site-scale simulations, we assumed a grid cell with single tile entirely covered by crops.

Relative root extractible soil moisture in the different soil layers was computed in each

hydrological scheme as the mean relative soil moisture over the different soil layers, weighted by the fraction of roots within each layer (Krinner et al., 2005). The stress index defined above was then calculated based on relative root extractible water, which differs between the 2LAY and the 11LAY versions. Irrigation was not taken into account in the current version of ORCHIDEE-CROP. The typical exponential (static) root profile assumed for grass and crop PFT in ORCHIDEE locates ~65% of the roots in the upper 20 cm of the soil. This root distribution profile was different from the one that was used in STICS, where fewer roots were assumed to be in the upper 20 cm of soil and more below (Brisson et al., 2008; Gervois et al., 2004). In ORCHIDEE-CROP we kept the root profile as parameterized in ORCHIDEE.

2.1.4 Simplified nitrogen limitation and fertilization effects

Nitrogen fertilization increases crop productivity and the LAI, which consequently impacts on crop phenology, carbon allocation, and turbulent fluxes exchanged with the atmosphere (Mueller et al., 2012). ORCHIDEE-CROP is currently unable to account for dynamic nitrogen stress within the crop growing season due to the lack of an explicit parameterization of nitrogen processes and nitrogen-carbon interactions. We thus defined a simple nitrogen limitation index (innlai) and expressed it as a parameter ranging from 0 (the maximum limitation of nitrogen) to 1 (without nitrogen limitation). To account, in a very simple manner, for the effects of nitrogen fertilization on plant productivity, we introduced an additive nitrogen response parameter, N_{add}, which is linked to photosynthetic parameters, V_{cmax_opt} and $J_{\max\_opt}$, using the following

equation:

$$N_{add} = 1 + N_{max} - N_{max} \times 0.75^{(N_{fert}/30)} \quad (2)$$

where N_{max} is the maximum additive effects of nitrogen fertilization during the growing season, N_{fert}, on the photosynthetic parameters (for details see Chang et al., 2015). The N_{max} is a PFT-specific parameter that can be calibrated by the observed additive nitrogen fertilization effects on plant productivity (e.g., using field trials). This simple function allowed us to estimate the impacts of different levels of nitrogen fertilization on crop productivity (Chang et al., 2015).

2.2 Simulation set-up

2.2.1 Site description

We tested ORCHIDEE-CROP using winter wheat and maize at seven eddy-covariance sites, which are part of the CarboEurope-IP project (http://www.carboeurope.org/). These sites span different climatic conditions (Table 1 and Fig S1). All the sites recorded the meteorological half-hourly variables necessary to run ORCHIDEE-CROP as well as CO_2 fluxes (NEE), and latent and sensible heat fluxes. The NEE half-hourly data were gap-filled and partitioned into gross primary productivity (GPP) and total ecosystem respiration (TER) using the online eddy covariance processing tool (Moffat et al., 2007; Papale, 2006; Reichstein et al., 2005). Management information (e.g., sowing and harvest date, irrigation and fertilization) and crop development monitoring data (e.g., LAI, aboveground biomass (AGB) and crop yield) were available for each site and were used either for parametrization (sowing date, fertilization) or evaluation

purposes. The geographic locations, climate regimes, and management information are provided in Table 1, Table 2, and Fig. S1. More details about the seven sites can be found in (Kutsch et al., 2010; Vitale et al., 2007).

2.2.2 Climate forcing data and atmospheric CO_2

At each site, meteorological forcing on a half-hour time step was used as a model input. This included air temperature, precipitation, wind speed, atmospheric water vapor pressure, shortwave and longwave incoming radiation, and mean near-surface atmospheric pressure. Annual CO_2 atmospheric concentration was derived from background atmospheric measurements. There were gaps in the meteorological data, mainly caused by instrumentation malfunction. Therefore, we reprocessed the data using standardized procedures for gap-filling and quality control (Moffat et al., 2007; Papale, 2006). A significant source of systematic errors in comparisons between modeled and eddy covariance fluxes were attributed to the lack of energy balance closure in the eddy covariance measurements (Foken, 2008). Our evaluation revealed an obvious problem regarding the energy balance closure in the eddy covariance observations on these crop sites where the energy closure rate ranged from ~ 80.6% to 86.3% (e.g., Fig. S2). We thus corrected the daily LE and H measurements in a similar way to Twine *et al*. (Twine et al., 2000) and Jung *et al*. (Jung et al., 2011), which preserved the Bowen ratio:

$$E_{corr} = \alpha \times E_{uncorr} = (R_n - G)/(H_{uncorr} + LE_{uncorr}) \times E_{uncorr} \quad (3)$$

where, E is either the LE or H flux, α is a daily correction factor, and R_n and G are the net radiation and soil heat flux, respectively. In our correction, we do not consider the soil heat flux due to the lack of observations. Although the magnitude and causes of energy budget imbalance probably vary among sites and across time scales (Barr et al., 2006; Franssen et al., 2010), this simplified approach can correct the energy balance closure gap and yields consistent energy fluxes with other independent estimates (Jung et al., 2011).

2.2.3 Simulation experiments

A set of simulations were performed for each crop-site (Table 1) using STICS (JavaStics-v11, http://www6.paca.inra.fr/stics/), ORCHIDEE, and ORCHIDEE-CROP to evaluate the performance of ORCHIDEE-CROP and the impacts of the parameterizations of the nitrogen limitation factor and soil hydrology schemes (Table 3). Observed climate data and crop type at each site were used to drive the models (in ORCHIDEE, winter wheat is described by the C3 crop standard parameters and maize by the standard C4 crop ones). The same mean soil depth and soil water holding capacity were prescribed for the seven sites, and were averaged from the Harmonized World Soil Database (HWSD), http://webarchive.iiasa.ac.at/Research/LUC/External-World-soil-database/HTML/). For each site, we selected one year of observation during which winter wheat or maize was cultivated. The sowing date was inputted into the model for each crop-site according to the management data (Table 2). However, the harvest date in ORCHIDEE-CROP was determined by crop

development processes. The observed nitrogen fertilization and irrigation information for each crop-site were used in STICS experiment STI-WN (Table 2 and Table 3). In STICS, the real date and quantity of applied irrigation and nitrogen fertilization can be introduced into the model, which affects the water balance and nitrogen transformation modules, respectively (Brisson et al., 2008).

All simulations based on ORCHIDEE and ORCHIDEE-CROP started from an equilibrium state of carbon pools where the climate was obtained using a model spin-up. For this spin-up, site-specific meteorological half-hourly data was repeatedly cycled for 300 years to force ORCHIDEE and ORCHIDEE-CROP until the soil water reached a steady state (data not shown). Then, simulations were conducted for the period of evaluation, starting from the initial conditions at the end of model spin-up. Notably, C input from manure applications was not taken into account in this study due to a lack of data for historical manure applications.

The same cultivar choice (represented by the "Soissons" and "DK250" variety parameters in STICS for winter wheat and maize, respectively), rather than site-year specific varieties, was made at all sites for winter wheat and maize (see Table 3). This may lead to some discrepancies between simulated and observed values, but our main purpose was to evaluate the improvements achieved by ORCHIDEE-CROP in a generic way, without having to calibrate the model for each site. Sensitivity tests were conducted to evaluate the effects of nitrogen limitation and water stress on crop development, carbon, and energy budgets. The experimental details are shown in Table 3.

414

415 **2.3 Metrics for evaluating model performance**

416 Three metrics were used to evaluate the model-data agreements at a daily resolution for
417 NEE, H, and LE fluxes, and the LAI, AGB, and grain yield biometric variables.

418 First, we calculated the index of agreement (IOA) (Willmott et al., 1985), given by

419 $$\mathrm{IOA} = 1.0 - \sum_{i=1}^{n}(O_i - P_i)^2 / \sum_{i=1}^{n}(|P_i - \bar{O}| + |O_i - \bar{O}|)^2 \quad (4)$$

420 where P_i is the modelled data, O_i is the observed data, $\bar{O}$ is the observed mean and
421 n is the numbers of data. The IOA, with values ranging from 0.0 to 1.0, is more
422 sensitive than correlation-based metrics to differences in the observed and modelled
423 means and variances (Willmott et al., 1985).

424 We also calculated the Pearson's product-moment correlation coefficient for all sites.
425 This metric estimates the proportion of total variance in the observed data that can be
426 explained by model, and is given by

427 $$r = \frac{\sum_{i=1}^{n}(P_i - \bar{P})(O_i - \bar{O})}{\sqrt{\sum_{i=1}^{n}(P_i - \bar{P})^2}\sqrt{\sum_{i=1}^{n}(O_i - \bar{O})^2}} \quad (5)$$

428 where $\bar{P}$ is the modeled mean.

429 Third, the root mean square error (RMSE) and normalized root mean square error
430 (NRMSE) were used to quantify the model-observation agreement in absolute terms,
431 expressed as

432 $$\mathrm{RMSE} = \sqrt{\sum_{i=1}^{n}(P_i - O_i)^2 / n} \quad (6)$$

433 and $$\mathrm{NRMSE} = \sqrt{\sum_{i=1}^{n}(P_i - O_i)^2 / n} / (O_{max} - O_{min}) \quad (7)$$

434 where and $Omax$ and $Omin$ are observed maximum and minimum data.

3. Results

3.1 Crop phenology, plant development stages and productivity

Comparison of the seasonal evolution of observed and modelled LAI for winter wheat and maize at different sites was shown in Fig. 2. The modelled seasonality for LAI has been markedly improved by ORCHIDEE-CROP (ORC-CP1, Table 3) compared to ORCHIDEE, for both winter wheat and maize. The correlation coefficient between observed daily LAI and modelled daily LAI increased from 0.44 ± 0.22 to 0.83 ± 0.17 for winter wheat and from 0.64 ± 0.22 to 0.79 ± 0.10 for maize from ORCHIDEE to ORCHIDEE-CROP (ORC-CP1), respectively. The IOA increased from 0.47 ± 0.11 to 0.82 ± 0.12 (winter wheat) and from 0.57 ± 0.15 to 0.85 ± 0.08 (maize), with a significant decrease in RMSE (2.71 ± 0.49 vs. 1.12 ± 0.36 and 2.06 ± 0.86 vs. 1.04 ± 0.31 for winter wheat and maize, respectively) (Fig. 2, Table 4, Fig. 5a–b). Despite its overall good performance for LAI, ORC-CP1 (under moderate nitrogen limitation of leaf growth) could not reproduce the observed LAI within the measurement uncertainty (personal communications with PIs in 2014) at a few sites (Fig. 2). For example, maximum LAI was underestimated by 49% and 28% for winter wheat at FR-Gri and FR-Lam, respectively. Reducing the nitrogen limitation of leaf growth (ORC-CP3) at these two sites could improve the modelled maximum LAI and bring it into agreement with the observations (Fig. S3, Table 4). The modelled growing season length (defined as the period from crop sowing to harvest) by ORC-CP1 for all crop sites was in good

agreement with the observations (IOA = 0.96 and RMSE = 25.4 days) (Fig. 3). The accurately simulated timing and amplitude of LAI improved the seasonal evolution of aboveground biomass (AGB) in ORCHIDEE-CROP (ORC-CP1) compared to ORCHIDEE for both winter wheat and maize, except at BE-Lon for winter wheat and at NL-Lan for maize (Fig. 4, Fig. 5). In general, the bias of the modelled AGB was attributable to the bias in the modelled LAI as indicated by the significant ($p < 0.005$) relationship between AGB and LAI for all sites (Fig. S4). However, the daily change rate of above-ground biomass in the late growing season between the start of grain filling and yield harvest was systematically and significantly ($p < 0.05$) underestimated for both winter wheat (change rate of AGB underestimated by 36%–74%) and maize (18%–70%), especially at the sites where LAI was underestimated (e.g., winter wheat at FR-Gri and FR-Lam) (Fig. 2, Fig. 4, Fig. S5). The observation data did not show a decrease in above-ground biomass until harvest (Fig. 4).

ORCHIDEE-CROP (ORC-CP1) could capture the timing of grain filling and yield harvest well compared to the observations and STICS simulations (Fig. S6). Comparisons of modelled and observed crop yields for winter wheat and maize in FR-Aur and FR-Lam showed that there was a 19% to 30% underestimation of crop yields in ORC-CP1 without fertilization (Fig. 6), compared to a good match (NRMSE = ~8.8%) between STICS with real fertilization (STI-WN) and the observed data (Fig. S6). However ORCHIDEE-CROP with real fertilization (ORC-CP4) could produce a better estimation of crop yields for these two sites than ORCHIDEE-CROP without

fertilization (ORC-CP1), leading to a 50% reduction in the NRMSE (47% vs. 23% for ORC-CP1 vs. ORC-CP4, respectively) (Fig. 6). Considering the measurement uncertainties of FR-Aur and FR-Lam for crop yields (personal communications with PIs in 2014), ORCHIDEE-CROP, with its simple nitrogen fertilization parameterization, generally showed reasonable performance compared to STICS, which has a complete nitrogen cycle and captures both the timing and amplitude of crop yields.

3.2 CO_2 and energy fluxes

ORCHIDEE-CROP had a more realistic simulated seasonality and amplitude for NEE at most of the winter wheat sites than ORCHIDEE (significant increase in IOA and *r* and decrease in RMSE from 2.9 ± 0.2 g C m^{-2} day^{-1} in ORCHIDEE to 1.9 ± 0.5 g C m^{-2} day^{-1} in ORC-CP1). Improved performances of ORCHIDEE-CROP over ORCHIDEE were also found at the maize sites in humid regions (Fig. S1, Fig. 7). Along with leaf area development during the growing season, the model produced a CO_2 sink until shortly before harvest, when most leaves were senescent and crop photosynthesis could not compensate for respiration, which was consistent with the observed data (Fig. 7). ORCHIDEE-CROP could also capture the observed peak in CO_2 release to atmosphere shortly (ranging from 10 to 20 days, Fig. 7) after harvest for both winter wheat and maize, which was mainly due to increased litter decomposition.

However, there was a mismatch between the simulations and observations regarding the temporal evolution of NEE for winter wheat in BE-Lon, where there was a weaker

and earlier termination of CO_2 uptake in the model (Fig. 7). The underestimated LAI and earlier cessation of crop growth in ORC-CP1 at this site resulted in a negative bias for GPP during the late growing season (~170 days after sowing) (Fig. 2, Fig. S7), which contributed to the underestimation of NEE uptake (Fig. 7, Fig. S8). Notably, ORC-CP1 overestimated the NEE peak uptake of CO_2 for maize at sites with drier climates in Europe (e.g., FR-Lam and IT-Bci). The overestimation of NEE at these summer-dry sites was probably (68%–85% of explained variance revealed by the General Linear Model) caused by an overestimation of GPP rather than by an underestimation of ecosystem respiration in ORC-CP1 (Fig. S7, Fig. S8). Further analysis showed a much higher ($p < 0.05$) rate for GPP per unit LAI in ORC-CP1 than observed at the southern maize sites (Fig. S9). Notably, ORCHIDEE-CROP with the 11-LAY hydrological scheme (ORC-CP5) improved the modelled NEE for maize at these sites because it showed a 40% decrease in the NRMSE (Fig. 7).

Despite the improved seasonality of H for most of the crop-sites over Europe (Fig. S10), ORCHIDEE-CROP with the 2LAY hydrological scheme generally overestimated H for winter wheat sites, especially in the early- and mid-growing season (from sowing to 160–200 days after sowing) and showed a more realistic simulation of H for maize sites (NRMSE of ~9%–13%). The overestimation of H at wheat sites occurred during the early- and mid-growing season (Fig. 8) when the plants were growing slowly with a low canopy cover. This could be partly attributed to the underestimation of soil water content in the top soil during that period (data not shown) or to the insufficiently deep roots prescribed in the model. Notably, the ORC-CP5 with the 11LAY soil hydrological

scheme, which had a more realistic representation of soil water infiltration after rain and could simulate the vertical profile of soil moisture with desiccation of the surface soil during dry episodes, improved the simulation of H during this period, with the NRMSE being brought down from 7%–10% in ORC-CP1 to 5%–8% in ORC-CP5 (Fig. 8). Notably, however, the 11LAY hydrological scheme usually overestimated the bare soil evaporation (data not shown), which would result in drier top soil conditions and lead to a higher H. This could partially explain the residual overestimation of H, even in ORC-CP5 (Fig. S10).

Consistent with the overestimation of H in ORC-CP1, LE was generally underestimated at the wheat sites (Fig. 9). A more realistic estimation of LE was obtained by ORC-CP5 for a majority of the sites, showing a 32% decrease in NRMSE from ORC-CP1 to ORC-CP5. The exceptions were the winter wheat and maize simulation at the DE-Kli site, which could be attributed to a considerable energy balance gap (with an energy closure of ~73%) at this site (Fig. 9). For maize, ORC-CP5 overestimated LE at DE-Kli by ~110% compared to the observed data. The LE values were also overestimated for wheat during the early- and mid-growing season (from sowing to 230 days after sowing). The overestimation of LE at DE-Kli was not explained by the LAI bias (see above) nor by a systematic error in LE due to the effects of rainfall events (with daily rainfall $\geqslant$ 3 mm) (Figs. 8–9), but was possibly due to some other factors, such as soil water holding capacity. The slightly negative bias in LE simulated by ORC-CP5 at the wheat site FR-Lam during the peak leaf growth (210–250 days after planting) was due to an underestimation of the LAI (Fig. 9, Fig. 2). The slight overestimation of LAI for

maize during periods of peak leaf growth (e.g., FR-Lam and NL-Lan) did not translate into a related overestimation of LE. This illustrated the divergent responses of LE to changes in LAI between ORCHIDEE-CROP and the observations, which could be due to several factors, such as the parameterization of soil water stress (Fig. S11). The episodes of LE with low biases (during LE peaks) coincided with high H biases, even though net radiation appeared to be realistic, except for the maize site IT-Bci in Italy (Fig. S12).

ORCHIDEE-CROP could also capture the spatial gradients of carbon and energy fluxes across different crop sites in Europe. There were significant correlation coefficients between the observed and modelled GPP, NEE, H, and LE data, with *r* ranging from 0.75 to 0.90. Evaluation of IOA revealed a generally good agreement between the observed and modelled GPP, NEE, H, and LE data with IOA ranging from 0.70 to 0.90 (Fig. 10, Fig S14–S16).

4. Discussion

4.1 General performance of ORCHIDEE-CROP

ORCHIDEE-CROP has been developed as an Agro-LSM and adopts a generic framework to integrate the crop processes from STICS into the ORCHIDEE LSM. Given its generic structure, ORCHIDEE-CROP, tested using wheat and maize in this study, can simulate other crop types. Crop phenology, development, carbon allocation

565 and grain filling can be calculated from climate forcing data and is mediated by limiting
566 factors (e.g., nitrogen, extreme temperatures, and low soil moisture).
567 A significant improvement was obtained using ORCHIDEE-CROP compared to
568 ORCHIDEE for the simulated crop phenology and development at different winter
569 wheat and maize sites. It showed 65%–95% (IOA) for biometric data and 78%–98%
570 (IOA) agreement with the observed data for all turbulent fluxes, despite the lack of
571 detailed crop management (e.g., irrigation, fertilization) parameterization (Figs. 2–9)
572 and the lack of an explicit calculation for the nitrogen cycle in the croplands.
573 Remarkably, ORCHIDEE-CROP has a good ability to reproduce the observed spatial
574 gradients for carbon and energy fluxes across different climate zones in Europe, even
575 using a fixed variety parameter setting for different sites. This implied that these spatial
576 gradients in biophysical and biochemical variables are mainly driven by climate rather
577 than by crop variety.
578 Improvements in crop phenology and carbon allocation led to a general good match of
579 the seasonality between modelled and observed AGB (with NRMSEs of 11%–54%),
580 crop yields, and carbon and energy fluxes (NRMSEs of 9.0–20.1% and 9.4–22.3% for
581 NEE and sensible and latent heat fluxes, respectively). Comparisons between the 2LAY
582 and 11LAY hydrological schemes revealed that the 11LAY hydrological scheme can
583 improve the modelling of soil water dynamics and hence lead to a better simulation of
584 leaf growth and consequent biochemical and biophysical variables, especially for the
585 C4 crops planted in the drier climate zones of Europe (Fig. 7–9). This in turn exerts
586 great effects on the estimations of carbon balances in these regions, especially in the

context of the projected increasing climate variability and extremes (e.g., heat waves and drought events) (Beniston et al., 2007; Ciais et al., 2005; Stocker et al., 2013). Yet, parameterization of water stress also depends on the distribution of active roots, which is considered as fixed in all ORCHIDEE versions. The use of a static root profile is one limit on the calculation of water stress, but the use of 11-Layer hydrology allows us to simulate shifts in root uptake from the surface to deeper horizons as the soil dries out during drought. An important area for further research could be a more mechanistic parameterization of the root profile in the model.

Notably, the simple function of additive nitrogen fertilization on crop productivity can lead to better agreement between the observed and modelled crop yields in ORCHIDEE-CROP, which showed a 50% decrease in the NRMSE (Fig. 6). The remaining discrepancies in simulated crop yields and energy fluxes are generally within the observed uncertainties for measurement and energy balance closure. More importantly, ORCHIDEE-CROP has the ability to capture the spatial gradients of crop-related flux variables, such as GPP, NEE, H, and LE, across the studied sites in the different European climate zones (Fig. 10, Figs. S14–S16). This is important for further applications of this model using gridded data over Europe, or even the globe, when attempting to investigate regional/global yield variations and the interactions between croplands and the climate system. Croplands have potentially crucial climate feedbacks regarding the increased intensification of agricultural activities and land use changes (Pitman et al., 2009; Ramankutty et al., 2002; Sacks and Kucharik, 2011).

Failure of the model to capture the peak LAI at some crop sites (e.g., winter wheat at

609 FR-Gri and FR-Lam) under ORC-CP1 is partly attributed to the simplified
610 representation of nitrogen limitation on crop growth and fertilization effects (section 2).
611 Alleviation of nitrogen limitation on leaf growth at those sites can improve the
612 simulated amplitudes of LAI and capture the maximum LAI (Fig. S3). Nitrogen
613 limitation has a strong influence on the seasonal evolution of crop growth (Fig. S3). A
614 more realistic representation of intra-seasonal nitrogen processes (results based on
615 STICS with an explicit nitrogen cycle) leads to a generally much better match between
616 the modelled and observed LAI, except for NL-Lan and maize (Fig. S13).
617 The failure to model irrigation effects can also introduce some bias to the simulated
618 LAI and other variables. Soil water stress on GPP and LE, which also affects carbon
619 allocation, plays an important role in controlling crop development, especially for
620 summer crops (e.g., maize) planted in regions with dry summer episodes (Fig. S1, Table
621 1). Those regions are currently suffering from intensive irrigation management (Table
622 2) and there will possibly be an increase in irrigation requirements as the climate warms
623 (Döll, 2002). As illustrated by our results the lack of irrigation management in the
624 current version of ORCHIEE-CROP leads to a lower LAIs in the later crop season at
625 FR-Lam for maize in drier climate zones (Fig. 2 and Fig. 7), which, in turn, affect NEE
626 and the energy budget (Fig. 7–9). More importantly, the projected increased drought
627 stress for cultivated croplands (Dai, 2012), with a more intense and longer lasting
628 droughts in drier climate zones (Davin et al., 2014; Trenberth et al., 2014), challenges
629 the representations of soil hydro-logical processes and their interactions with other
630 factors for existing Agro-LSMs.

4.2 Model limitation and uncertainty

Irrigation (as discussed above) effects on the crop development and yields are not accounted for in the current version of ORCHIDEE-CROP, but it is important when attempting to investigate the historically long-term changes in crop yields over recent decades, as intensive human management has tended to occur since approximately the middle of the 20th century.

Several studies have shown that the spatial differences in crop management contribute significantly to the tempo-spatial patterns of crop yields (Licker et al., 2010; Lobell and Field, 2007), as well as the impacts of climate and soil fertility (Rosenzweig et al., 2013). Adaptive improvements in agricultural management are regarded as a potential way to close the "*yield gaps*" in a relatively sustainable manner (Licker et al., 2010). How the model handles human management factors (e.g., irrigation and fertilization) and their interactions with changing CO_2 and climate variations could have significant impacts on the crop production simulations and the consequent land surface carbon budgets (Prescher et al., 2010). Additionally, our current crop development module embodies a number of simplifications for pests, diseases, and weeds, which we assumed to be controlled. Extreme soil conditions (e.g., high salinity or acidity) are also crudely assumed to have little effect on crop growth. These factors can also introduce great uncertainties into the biophysical and biochemical simulations of croplands.

Therefore, explicit nutrition dynamics and a human management (e.g., irrigation, fertilization, introduction of new crop varieties, and pest management, etc.) module

need to be included in the updated version of ORCHIDEE-CROP to improve our ability to understand and project the roles of croplands in food security, environmental footprints and ecosystem services in response to climate change.

5. Conclusions

ORCHIDEE-CROP, by integrating a generic process-based crop development and yield harvest module into a generic LSM-ORCHIDEE program, allow us to assess the spatial and temporal dynamics of the important biophysical and biochemical interactions within the soil-vegetation-atmosphere continuum for temperate crops. Comprehensive evaluations show the generally good performance of ORCHIDEE-CROP at predicting crop phenology, productivity, and the biosphere-atmosphere carbon and energy exchanges in pan-Europe temperate crop sites covering different climate zones, even without the explicit human management module. It benefits from a generic strategy in the crop module, which makes ORCHIDEE-CROP widely applicable at the regional and global scale. Explicit parameterizations of crop development processes in ORCHIDEE-CROP can improve the simulations of both the seasonality and magnitudes of LAI for croplands, which in turn affect the consequent surface roughness, surface albedo, water, energy, and carbon budgets for land surfaces. Therefore, with respect to future climate change, ORCHIDEE-CROP will allow us to predict the footprints of climate variations on food security, and to simultaneously account for feedbacks caused by changes in crop behaviors to the atmosphere by coupling it to a

675 general atmospheric circulation model (e.g., LMDz).

676 Nevertheless, further improvement, especially with regards to explicit nutritional
677 dynamics and human management, is a primary priority and could significantly
678 improve our ability to understand and predict the role of croplands in the biosphere-
679 atmosphere continuum, in the context of the increasing global demand for food and the
680 urgent requirement to reduce the environmental footprints (Godfray et al., 2010;
681 Mueller et al., 2012).

682

683 **6. Acknowledgements**

684 We thank Dr. Jinfeng Chang, and Dr. Chao Yue from Laboratoire des Sciences du
685 Climat et de l'Environnement (LSCE) of France for their valuable help for Fortran
686 coding. This work was supported by the EU FP7 project GHG-Europe (Greenhouse gas
687 management in European land use systems; grant No. 244122).

688

689 **7. Code availability**

690 The ORCHIDEE-CROP is still undergoing development, especially for human
691 management processes, and the code is modified frequently. Therefore, the codes are
692 not ready for fully public access. However, the source codes of ORCHIDEE-CROP at
693 an early version (V0) can be requested from Xiuchen Wu (xiuchen.wu@bnu.edu.cn) or
694 Nicolas Vuichard (nicolas.vuichard@lsce.ipsl.fr).

695

References

Asseng, S., Ewert, F., Rosenzweig, C., Jones, J., Hatfield, J., Ruane, A., Boote, K., Thorburn, P., Rötter, R., and Cammarano, D.: Uncertainty in simulating wheat yields under climate change, Nature Climate Change, 3, 827-832, 2013.

Barr, A., Morgenstern, K., Black, T., McCaughey, J., and Nesic, Z.: Surface energy balance closure by the eddy-covariance method above three boreal forest stands and implications for the measurement of the CO_2 flux, Agricultural and Forest Meteorology, 140, 322-337, 2006.

Bassu, S., Brisson, N., Durand, J.-L., Boote, K., Lizaso, J., Jones, J. W., Rosenzweig, C., Ruane, A. C., Adam, M., Baron, C., Basso, B., Biernath, C., Boogaard, H., Conijn, S., Corbeels, M., Deryng, D., De Sanctis, G., Gayler, S., Grassini, P., Hatfield, J., Hoek, S., Izaurralde, C., Jongschaap, R., Kemanian, A. R., Kersebaum, K. C., Kim, S.-H., Kumar, N. S., Makowski, D., Müller, C., Nendel, C., Priesack, E., Pravia, M. V., Sau, F., Shcherbak, I., Tao, F., Teixeira, E., Timlin, D., and Waha, K.: How do various maize crop models vary in their responses to climate change factors?, Global Change Biology, 20, 2301-2320, 2014.

Beniston, M., Stephenson, D. B., Christensen, O. B., Ferro, C. A., Frei, C., Goyette, S., Halsnaes, K., Holt, T., Jylhä, K., and Koffi, B.: Future extreme events in European climate: an exploration of regional climate model projections, Climatic Change, 81, 71-95, 2007.

Berg, A., Sultan, B., and de Noblet-Ducoudré, N.: Including tropical croplands in a terrestrial biosphere model: application to West Africa, Climatic Change, 104, 755-782, 2011.

Bonan, G. B.: Forests and climate change: forcings, feedbacks, and the climate benefits of forests, Science, 320, 1444-1449, 2008.

Bonan, G. B.: Observational evidence for reduction of daily maximum temperature by croplands in the Midwest United States, Journal of Climate, 14, 2430-2442, 2001.

Bondeau, A., Smith, P. C., Zaehle, S., Schaphoff, S., Lucht, W., Cramer, W., Gerten, D., LOTZE‐CAMPEN, H., Müller, C., and Reichstein, M.: Modelling the role of

725 agriculture for the 20th century global terrestrial carbon balance, Global Change
726 Biology, 13, 679-706, 2007.
727 Brisson, N., Launay, M., Mary, B., and Beaudoin, N.: *Conceptual basis, formalisations*
728 *and parameterization of the STICS crop model*, Edition Quae, Versailles Cedex,
729 2008.
730 Brisson, N., Mary, B., Ripoche, D., Jeuffroy, M. H., Ruget, F., Nicoullaud, B., Gate, P.,
731 Devienne-Barret, F., Antonioletti, R., and Durr, C.: STICS: a generic model for
732 the simulation of crops and their water and nitrogen balances. I. Theory and
733 parameterization applied to wheat and corn, Agronomie, 18, 311-346, 1998.
734 Brisson, N., Ruget, F., Gate, P., Lorgeou, J., Nicoullaud, B., Tayot, X., Plenet, D.,
735 Jeuffroy, M.-H., Bouthier, A., and Ripoche, D.: STICS: a generic model for
736 simulating crops and their water and nitrogen balances. II. Model validation for
737 wheat and maize, Agronomie, 22, 69-92, 2002.
738 Chang, J., Viovy, N., Vuichard, N., Ciais, P., Campioli, M., Klumpp, K., Martin, R.,
739 Leip, A., and Soussana, J.: Modelled changes in potential grassland productivity
740 and in ruminant livestock density in Europe over 1961-2010, PLoS One, 10,
741 e0127554, doi:10.1371/journal.pone.0127554554, 2015.
742 Ciais, P., Gervois, S., Vuichard, N., Piao, S., and Viovy, N.: Effects of land use change
743 and management on the European cropland carbon balance, Global Change
744 Biology, 17, 320-338, 2011.
745 Ciais, P., Reichstein, M., Viovy, N., Granier, A., Ogée, J., Allard, V., Aubinet, M.,
746 Buchmann, N., Bernhofer, C., and Carrara, A.: Europe-wide reduction in primary
747 productivity caused by the heat and drought in 2003, Nature, 437, 529-533, 2005.
748 Collatz, G. J., Ribas-Carbo, M., and Berry, J.: Coupled photosynthesis-stomatal
749 conductance model for leaves of C4 plants, Functional Plant Biology, 19, 519-538,
750 1992.
751 Döll, P.: Impact of climate change and variability on irrigation requirements: a global
752 perspective, Climatic Change, 54, 269-293, 2002.
753 Dai, A.: Increasing drought under global warming in observations and models, Nature
754 Climate Change, 3, 52-58, 2012.

Davin, E. L., Seneviratne, S. I., Ciais, P., Olioso, A., and Wang, T.: Preferential cooling of hot extremes from cropland albedo management, Proceedings of the National Academy of Sciences of the United States of America, 111, 9757-9761, 2014.

de Noblet-Ducoudré, N., Gervois, S., Ciais, P., Viovy, N., Brisson, N., Seguin, B., and Perrier, A.: Coupling the soil-vegetation-atmosphere-transfer scheme ORCHIDEE to the agronomy model STICS to study the influence of croplands on the European carbon and water budgets, Agronomie, 24, 397-407, 2004.

Farquhar, G., von Caemmerer, S. v., and Berry, J.: A biochemical model of photosynthetic CO_2 assimilation in leaves of C3 species, Planta, 149, 78-90, 1980.

Foken, T.: The energy balance closure problem: An overview, Ecological Applications, 18, 1351-1367, 2008.

Foley, J. A., Ramankutty, N., Brauman, K. A., Cassidy, E. S., Gerber, J. S., Johnston, M., Mueller, N. D., O'Connell, C., Ray, D. K., and West, P. C.: Solutions for a cultivated planet, Nature, 478, 337-342, 2011.

Franssen, H., Stöckli, R., Lehner, I., Rotenberg, E., and Seneviratne, S.: Energy balance closure of eddy-covariance data: A multisite analysis for European FLUXNET stations, Agricultural and Forest Meteorology, 150, 1553-1567, 2010.

Friedlingstein, P., Joel, G., Field, C., and Fung, I.: Toward an allocation scheme for global terrestrial carbon models, Global Change Biology, 5, 755-770, 1999.

Georgescu, M., Lobell, D., and Field, C.: Potential impact of US biofuels on regional climate, Geophysical Research Letters, 36, L21806, doi: 10.1029/2009GL040477, 2009.

Gervois, S., Ciais, P., de Noblet‐Ducoudré, N., Brisson, N., Vuichard, N., and Viovy, N.: Carbon and water balance of European croplands throughout the 20th century, Global Biogeochemical Cycles, 22, GB2022, doi: 10.1029/2007GB003018, 2008.

Gervois, S., de Noblet-Ducoudré, N., Viovy, N., Ciais, P., Brisson, N., Seguin, B., and Perrier, A.: Including croplands in a global biosphere model: methodology and evaluation at specific sites, Earth Interactions, 8, 1-25, 2004.

Godfray, H. C. J., Beddington, J. R., Crute, I. R., Haddad, L., Lawrence, D., Muir, J. F., Pretty, J., Robinson, S., Thomas, S. M., and Toulmin, C.: Food security: the

challenge of feeding 9 billion people, Science, 327, 812-818, 2010.

Guimberteau, M., Ciais, P., Ducharne, A., Boisier, J., Peng, S., De Weirdt, M., and Verbeeck, H.: Two soil hydrology formulations of ORCHIDEE (version Trunk. rev1311) tested for the Amazon basin, Geoscientific Model Development, 7, 1115-1136, 2014.

IPCC: Climate Change 2014: Impacts, Adaptation, and Vulnerability. Cambridge, United Kingdom and New York, NY, USA, 2014.

Jung, M., Reichstein, M., Margolis, H. A., Cescatti, A., Richardson, A. D., Arain, M. A., Arneth, A., Bernhofer, C., Bonal, D., Chen, J., Gianelle, D., Gobron, N., Kiely, G., Kutsch, W., Lasslop, G., Law, B. E., Lindroth, A., Merbold, L., Montagnani, L., Moors, E. J., Papale, D., Sottocornola, M., Vaccari, F., and Williams, C.: Global patterns of land-atmosphere fluxes of carbon dioxide, latent heat, and sensible heat derived from eddy covariance, satellite, and meteorological observations, Journal of Geophysical Research: Biogeosciences, 116, G00J07, doi:10.1029/2010JG001566, 2011.

Krinner, G., Viovy, N., de Noblet‐Ducoudré, N., Ogée, J., Polcher, J., Friedlingstein, P., Ciais, P., Sitch, S., and Prentice, I. C.: A dynamic global vegetation model for studies of the coupled atmosphere‐biosphere system, Global Biogeochemical Cycles, 19, GB1015, doi: 10.1029/2003GB002199, 2005.

Kucharik, C. J.: Evaluation of a process-based agro-ecosystem model (Agro-IBIS) across the US corn belt: simulations of the interannual variability in maize yield, Earth Interactions, 7, 1-33, 2003.

Kutsch, W., Aubinet, M., Buchmann, N., Smith, P., Osborne, B., Eugster, W., Wattenbach, M., Schrumpf, M., Schulze, E., and Tomelleri, E.: The net biome production of full crop rotations in Europe, Agriculture, Ecosystems & Environment, 139, 336-345, 2010.

Licker, R., Johnston, M., Foley, J. A., Barford, C., Kucharik, C. J., Monfreda, C., and Ramankutty, N.: Mind the gap: how do climate and agricultural management explain the 'yield gap'of croplands around the world?, Global Ecology and Biogeography, 19, 769-782, 2010.

Loarie, S. R., Lobell, D. B., Asner, G. P., Mu, Q., and Field, C. B.: Direct impacts on local climate of sugar-cane expansion in Brazil, Nature Climate Change, 1, 105-109, 2011.

Lobell, D., Bala, G., and Duffy, P.: Biogeophysical impacts of cropland management changes on climate, Geophysical Research Letters, 33, L06708, doi: 10.1029/2005GL025492, 2006.

Lobell, D. B. and Field, C. B.: Global scale climate–crop yield relationships and the impacts of recent warming, Environmental Research Letters, 2, 014002, doi:10.1088/1748-9326/2/1/014002, 2007.

Lobell, D. B., Schlenker, W., and Costa-Roberts, J.: Climate trends and global crop production since 1980, Science, 333, 616-620, 2011.

Müller, C.: Agriculture: Harvesting from uncertainties, Nature Climate Change, 1, 253-254, 2011.

Moffat, A. M., Papale, D., Reichstein, M., Hollinger, D. Y., Richardson, A. D., Barr, A. G., Beckstein, C., Braswell, B. H., Churkina, G., and Desai, A. R.: Comprehensive comparison of gap-filling techniques for eddy covariance net carbon fluxes, Agricultural and Forest Meteorology, 147, 209-232, 2007.

Mueller, N. D., Gerber, J. S., Johnston, M., Ray, D. K., Ramankutty, N., and Foley, J. A.: Closing yield gaps through nutrient and water management, Nature, 490, 254-257, 2012.

Osborne, T., Slingo, J., Lawrence, D., and Wheeler, T.: Examining the interaction of growing crops with local climate using a coupled crop–climate model, Journal of Climate, 22, 1393-1411, 2009.

Papale, D.: Towards a standardized processing of Net Ecosystem Exchange measured with eddy covariance technique: algorithms and uncertainty estimation, Biogeosciences, 3, 571-583, 2006.

Parry, M., Rosenzweig, C., and Livermore, M.: Climate change, global food supply and risk of hunger, Philosophical Transactions of the Royal Society B: Biological Sciences, 360, 2125-2138, 2005.

844 Pitman, A., de Noblet‐Ducoudré, N., Cruz, F., Davin, E., Bonan, G., Brovkin, V.,
845 Claussen, M., Delire, C., Ganzeveld, L., and Gayler, V.: Uncertainties in climate
846 responses to past land cover change: First results from the LUCID intercomparison
847 study, Geophysical Research Letters, 36, L14814, doi: 10.1029/2009GL039076,
848 2009.
849 Prescher, A.-K., Grünwald, T., Bernhofer, C.: Land use regulates carbon budgets in
850 eastern Germany: From NEE to NBP. Agricultural and Forest Meteorology, 150,
851 1016-1025, 2010.
852 Ramankutty, N. and Foley, J. A.: Characterizing patterns of global land use: An analysis
853 of global croplands data, Global Biogeochemical Cycles, 12, 667-685, 1998.
854 Ramankutty, N., Foley, J. A., and Olejniczak, N. J.: People on the land: Changes in
855 global population and croplands during the 20th century, AMBIO: A Journal of
856 the Human Environment, 31, 251-257, 2002.
857 Reichstein, M., Falge, E., Baldocchi, D., Papale, D., Aubinet, M., Berbigier, P.,
858 Bernhofer, C., Buchmann, N., Gilmanov, T., and Granier, A.: On the separation of
859 net ecosystem exchange into assimilation and ecosystem respiration: review and
860 improved algorithm, Global Change Biology, 11, 1424-1439, 2005.
861 Rosenzweig, C., Elliott, J., Deryng, D., Ruane, A. C., Müller, C., Arneth, A., Boote, K.
862 J., Folberth, C., Glotter, M., and Khabarov, N.: Assessing agricultural risks of
863 climate change in the 21st century in a global gridded crop model intercomparison,
864 Proceedings of the National Academy of Sciences of the United States of America,
865 111, 3268-3273, 2014.
866 Rosenzweig, C. and Parry, M. L.: Potential impact of climate change on world food
867 supply, Nature, 367, 133-138, 1994.
868 Sacks, W. J. and Kucharik, C. J.: Crop management and phenology trends in the US
869 Corn Belt: Impacts on yields, evapotranspiration and energy balance, Agricultural
870 and Forest Meteorology, 151, 882-894, 2011.
871 Sellers, W. D.: Physical Climatology, University of Chicago Press, Chicago, IL, 1965,
872 272p.
873 Stocker, T., Qin, D., Plattner, G., Tignor, M., Allen, S., Boschung, J., Nauels, A., Xia,

874 Y., Bex, V., and Midgley, P.: IPCC, 2013: Climate Change 2013: The Physical
875 Science Basis. Contribution of Working Group I to the Fifth Assessment Report
876 of the Intergovernmental Panel on Climate Change. Cambridge Univ Press,
877 Cambridge, United Kingdom and New York, NY, USA, 2013.
878 Trenberth, K. E., Dai, A., van der Schrier, G., Jones, P. D., Barichivich, J., Briffa, K. R.,
879 and Sheffield, J.: Global warming and changes in drought, Nature Climate Change,
880 4, 17-22, 2014.
881 Tubiello, F. N., Soussana, J.-F., and Howden, S. M.: Crop and pasture response to
882 climate change, Proceedings of the National Academy of Sciences of the United
883 States of America, 104, 19686-19690, 2007.
884 Twine, T. E., Kustas, W., Norman, J., Cook, D., Houser, P., Meyers, T., Prueger, J.,
885 Starks, P., and Wesely, M.: Correcting eddy-covariance flux underestimates over
886 a grassland, Agricultural and Forest Meteorology, 103, 279-300, 2000.
887 Valade, A., Ciais, P., Vuichard, N., Viovy, N., Huth, N., Marin, F., and Martiné, J.-F.:
888 Modeling sugar cane yield with a process-based model from site to continental
889 scale: uncertainties arising from model structure and parameter values,
890 Geoscientific Model Development, 7, 1225-1245, 2014.
891 Van den Hoof, C., Hanert, E., and Vidale, P. L.: Simulating dynamic crop growth with
892 an adapted land surface model–JULES-SUCROS: Model development and
893 validation, Agricultural and Forest Meteorology, 151, 137-153, 2011.
894 Vitale, L., Di Tommasi, P., Arena, C., Fierro, A., Virzo De Santo, A., and Magliulo, V.:
895 Effects of water stress on gas exchange of field grown *Zea mays L*. in Southern
896 Italy: an analysis at canopy and leaf level, Acta Physiologiae Plantarum, 29, 317-
897 326, 2007.
898 Vuichard, N., Ciais, P., Belelli, L., Smith, P., and Valentini, R.: Carbon sequestration
899 due to the abandonment of agriculture in the former USSR since 1990, Global
900 Biogeochemical Cycles, 22, GB4018, doi: 10.1029/2008GB003212, 2008.
901 Willmott, C. J., Ackleson, S. G., Davis, R. E., Feddema, J. J., Klink, K. M., Legates, D.
902 R., O'Donnell, J., and Rowe, C. M.: Statistics for the evaluation and comparison
903 of models, Journal of Geophysical Research: Oceans, 90, 8995-9005, 1985.

Tables

Table 1. Basic geography and climate information for different crop sites.

Crop type	SiteID	Country	MAP *	MAT †	Longitude	Latitude	Altitude (m)	KGCC ǂ
Winter wheat	FR-Lam	France	702	12.55	1.24	43.49	180	Cfb
	FR-Gri	France	579	11.5	1.95	48.84	125	Cfb
	FR-Aur	France	700	12.9	1.11	43.55	242.5	Cfb
	DE-Kli	Germany	674	7.1	13.52	50.89	478	Cfb
	Be-Lon	Belgium	800	10	4.74	50.55	165	Cfb
Maize	FR-Lam	France	702	12.55	1.24	43.49	180	Cfb
	FR-Gri	France	700	11.5	1.95	48.84	125	Cfb
	DE-Kli	Germany	674	7.1	13.52	50.89	478	Cfb
	NL-Lan	Netherland	786	9.8	4.9	51.95	-0.7	Cfb
	IT-Bci	Italy	900	15.5	14.96	40.52	20	Csa

Note:

* MAP: mean annual precipitation;

† MAT: mean annual temperature;

ǂ KGCC, the Koppen-Geiger climate classifications.

914 Table 2. Management information for different crop-sites.

915

Crop type	SiteID	Year (sowing)	Sowing date	Irrigation (mm)					Fertilization (Kg N/ha)			
Winter wheat	FR-Lam	2006	291	0	0	0	0	0	46.5 (8 Jan 2007)	48.2 (4 May 2007)	\	\
	FR-Gri	2005	301	0	0	0	0	0	55.0 (15 Mar 2006)	55.0 (14 Apr 2006)	\	\
	FR-Aur	2005	300	0	0	0	0	0	50.0 (25 Jan 2006)	40.0 (23 Mar 2006)	33.5 (12 Apr 2006)	\
	DE-Kli	2006	269	0	0	0	0	0	74.3 (8 Apr 2007)	53.8 (4 May 2007)	35.8 (4 Jun 2007)	43.1 (22 Jun 2007)
	Be-Lon	2006	286	0	0	0	0	0	40.0 (17 Mar 2007)	60.0 (12 Apr 2007)	94.5 (8 May 2007)	\
Maize	FR-Lam	2006	121	25.0 (13 Jun 2006)	33.0 (3 Jul 2006)	27.8 (15 Jul 2006)	18.0 (26 Jul 2006)	44.0 (10 Aug 2006)	91.0 (8 Jun 2006)	\	\	\
	FR-Gri	2005	129	0	0	0	0\	0	140.0 (9 May 2005)	\	\	\
	DE-Kli	2007	118	0	0	0	0	0	17.3 (22 Apr 2007))	67.2 (13 Jun 2007)	\	\
	NL-Lan*	2005	138	0	0	0	0	0	\	\	\	\
	IT-Bci	2004	129	21.8 (24 Jun 2004) 22.1 (27 Jul 2004)	27.2 (2 Jul 2004) 19.3 (31 Jul 2004)	20.3(15 Jul 2004) 22.9 (5 Aug 2004)	25.7 (18 Jul 2004) 22.1 (12 Aug 2004)	23.4 (20 Jul 2004) 15.0 (21 Aug 2004)	22.5 (8 May 2004)	142.0 (11 Jun 2004)	\	\

916 Note: * There is strong organic fertilization. \ indicates no fertilization records.

917

918

Table 3. Description of the ensemble of simulations.

Name of experiments	Description of experiments	Irrigation	Nitrogen processes *	Soil water scheme ǂ	Stlevdrp (GDD) ¶	Stdrpmat (GDD) ‼
STI-NN	STICS without fertilization during crop development ‖	NO	DY	\	540/990	750/600
STI-WN	STICS with actual fertilization based on management records !	NO	DY	\	540/990	750/600
ORC-ST0	Standard version of ORCHIDEE without crop development module, no fertilization	NO	NO	LAY2	540/990	750/600
ORC-CP1	ORCHIDEE-CROP with moderate nitrogen limitation, no fertilization	NO	NO, innlai = 0.5	LAY2	540/990	750/600
ORC-CP2	ORCHIDEE-CROP with high nitrogen limitation, no fertilization	NO	NO, innlai = 0.2	LAY2	540/990	750/600
ORC-CP3	ORCHIDEE-CROP with low nitrogen limitation, no fertilization	NO	NO, innlai = 0.9	LAY2	540/990	750/600
ORC-CP4	ORCHIDEE-CROP with moderate nitrogen limitation, real fertilization	NO	ND, innlai = 0.5	LAY2	540/990	750/600
ORC-CP5	Same to ORC-CP1, but with 11 layer soil hydrological scheme, no fertilization	NO	NO, innlai = 0.5	LAY11	540/990	750/600

Note:

* DY, with dynamic nitrogen processes, NO, without nitrogen processes, ND, without dynamic nitrogen processes but with a simplified additive nitrogen response of crop productivity to fertilization. For ORCHIDEE-CROP, we introduced a fixed nitrogen limitation factor for leaf growth (innlai, ranging 0.0-1.0) during the whole crop growing season.

ǂ Two soil hydrological schemes (the 2 layer soil scheme, referred as 2LAY, and the 11 layer soil diffusion scheme, referred as 11LAY, in detail see Guimberteau *et al.*, (2014)) are available in ORCHIDEE and ORCHIDEE-CROP.

¶ The accumulated growing degree days (GDD) from crop emergence to start of grain filling for winter wheat (C3 crop) and grain (C4 crop), respectively.

‼ The accumulated growing degree days (GDD) from start of grain filling to crop mature for winter wheat (C3 crop) and grain (C4 crop), respectively.

‖ JavaStics (v11.0) used here was obtained from http://www6.paca.inra.fr/stics.

! The detailed crop managements for each crop-site were shown in Table 2.

Table 4. Comparisons between observations and different simulations.

Crops	SiteID	IOA				R				RMSE (m^2 m^{-2})				NRMSE (%)			
		ORC-ST0	ORC-CP1	ORC-CP2	ORC-CP3	ORC-ST0	ORC-CP1	ORC-CP2	ORC-CP3	ORC-ST0	ORC-CP1	ORC-CP2	ORC-CP3	ORC-ST0	ORC-CP1	ORC-CP2	ORC-CP3
Winter wheat	BE-Lon	0.37	0.65	0.52	0.63	0.15	0.92**	0.98***	0.73	3.30	1.53	1.78	1.74	93.52	52.81	61.41	60.14
	FR-Lam	0.48	0.88	0.67	0.88	0.30	0.79*	0.83**	0.86**	2.68	0.90	1.48	1.21	60.72	20.44	33.52	27.56
	FR-Gri	0.66	0.87	0.63	0.97	0.74	0.96**	0.92*	0.97**	1.86	1.34	2.45	0.73	30.44	22.01	40.09	11.93
	FR-Aur	0.40	0.95	0.77	0.75	0.51	0.95**	0.91*	0.89*	3.06	0.52	0.85	1.58	107.47	18.42	29.84	55.61
	DE-Kli	0.46	0.74	0.56	0.62	0.49	0.55	0.47	0.56	2.68	1.31	1.17	2.07	101.02	49.26	44.06	77.96
Maize	DE-Kli	0.65	0.89	0.64	0.81	0.77	0.80*	0.74	0.89*	1.66	1.05	1.94	1.90	35.78	22.62	41.93	40.94
	FR-Lam	0.50	0.86	0.69	0.57	0.92*	0.76*	0.88*	0.55	2.46	1.00	1.31	2.58	74.95	30.42	40.08	78.75
	FR-Gri	0.58	0.96	0.64	0.91	0.45	0.95**	0.92**	0.97***	2.04	0.68	2.07	1.34	44.69	14.86	45.32	29.43
	NL-Lan	0.77	0.80	0.63	0.39	0.80	0.71	0.83*	0.45	0.79	0.89	1.34	2.52	24.82	27.98	42.28	79.18
	IT-Bci	0.38	0.74	0.49	0.73	0.42	0.70*	0.84*	0.65	3.37	1.60	2.62	1.98	85.37	40.59	66.33	50.11

Note: IOA, index of agreement; R, Pearson’s product-moment correlation coefficients; RMSE and NRMSE are the root mean square error and normalized root mean square error, respectively.

*, ** and *** indicates statistically significant at 5%, 1% and 1‰ level, respectively.

Figure captions

Figure 1. Model structures of the ORCHIDEE-CROP. The crop development module (based mainly on STICS, (Brisson *et al*., 1998)) is integrated into the STOMATE module of ORCHIDEE (Krinner *et al*., 2005). The crop development module simulated the phenology, developments and grain yields for crop PFTs. ORCHIDEE-CROP consists in the coupling of two modules. SECHIBA simulates the vegetation photosynthesis, water and energy budgets, STOMATE is a carbon module and calculates carbon allocation in different carbon pools and fluxes to the atmosphere.

Figure 2. Temporal changes of daily leaf area index (LAI) since planting from observations (green dots), standard ORCHIDEE (ORC-ST0, grey line) and ORCHIDEE-CROP (ORC-CP1, orange line). The upper and lower panel shows the results for different sites of winter wheat and maize, respectively.

Figure 3. Comparisons of the observed and modelled (ORC-CP1, in detail see Table 3) growing season lengths (from sowing to maturity) for winter wheat and maize in

962 different sites. Different colors indicate data for different crop-sites.

963

964

965 Figure 4. Comparisons of the observed (green dots) and modelled daily aboveground
966 biomass from ORCHIDEE-CROP (ORC-CP1, orange line) and ORCHIDEE (ORC-
967 ST0, grey line) for winter wheat and maize in different sites. The upper and lower panel
968 shows the results for different sites of winter wheat and maize, respectively.

969

970 Figure 5. Scatter plots of the modeled (ORC-CP1, in detail see Table 3) and observed
971 daily LAI and aboveground biomass (AGB) for different sites of winter wheat (a and c)
972 and maize (b and d), respectively. The units for RMSE of LAI and AGB are m^2 m^{-2} and
973 g C m^{-2}, respectively. Different colors indicate different crop-sites with red, orange,
974 light green, green and dark green for winter wheat (-W) at BE-Lon, DE-Kli, FR-Aur,
975 FR-Gri and FR-Lam, respectively, and with light blue, medium blue, blue, purple and
976 violet for maize (-M) at DE-Kli, FR-Gri, FR-Lam, IT-Bci and NL-Lan, respectively.

977

978

979 Figure 6. Comparisons of the observed (blue bars) and modelled (green bars for ORC-
980 CP1 and brown bars for ORC-CP4, see Table 3) harvested crop yields in different sites
981 for winter wheat a) and maize b).

982

983 Figure 7. Temporal changes of daily net ecosystem exchanges (NEE) derived from
984 observations (black line) and ORCHIDEE-CROP (ORC-CP1, blue line; ORC-CP5,
985 brown line) since planting. The green and blue stems represent the fertilization (kg N
986 ha^{-1}) and irrigation (mm) events during the selected growing season. The dotted orange
987 line indicates the harvest date since planting. The upper and lower panel shows the
988 results for different sites of winter wheat and maize, respectively.
989
990 Figure 8. Comparisons between the observed (black line) and modeled daily sensible
991 heat fluxes (H) from ORCHIDEE-CROP (ORC-CP1, blue line; ORC-CP5, brown line)
992 for different crop-sites. The grey stems represent the relative large rainfall events (with
993 daily summed rainfall $\geqslant$ 3 mm) during the modelled growing season. The upper and
994 lower panel shows the results for different sites of winter wheat and maize, respectively.
995
996
997 Figure 9. Same to Figure 8 except for latent heat fluxes (LE).
998
999 Figure 10. Comparisons between the observed and modelled (based on ORC-CP5)
1000 mean growing season GPP among different crop sites for winter wheat (circle, -W) and
1001 maize (cross, -M). Different colors indicate different sites.
1002
1003

Figures

Fig. 1

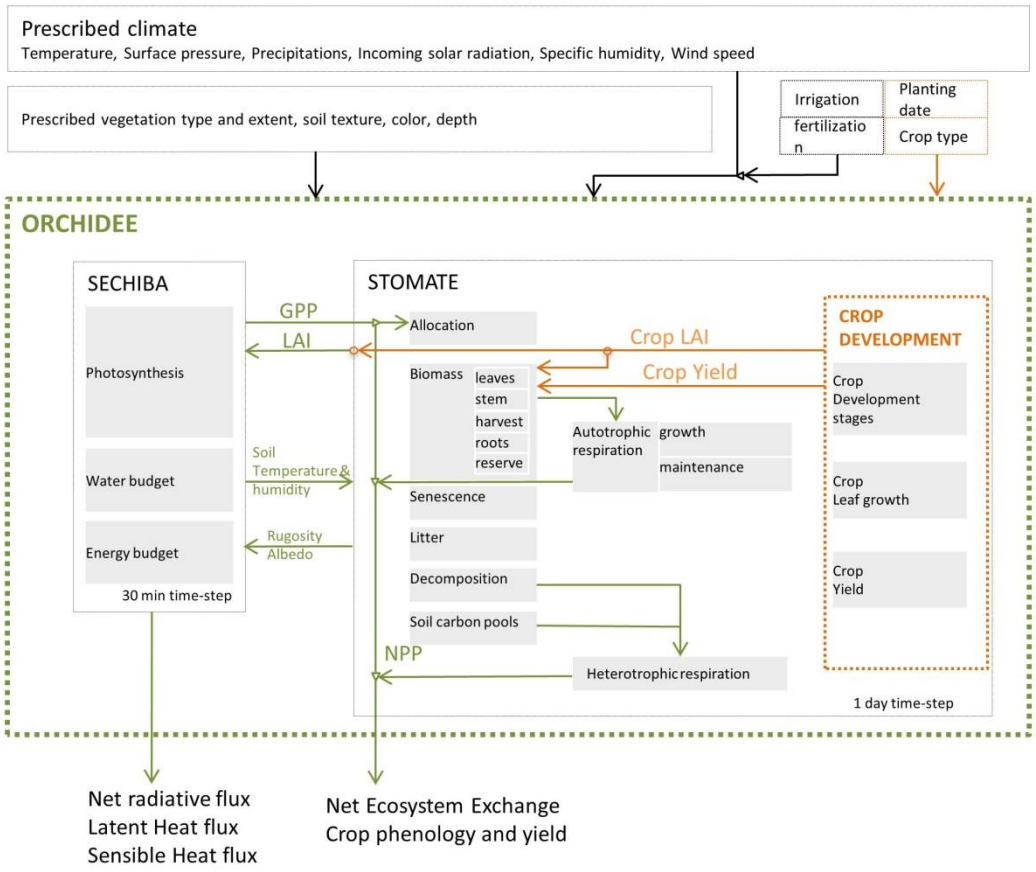

Fig. 2

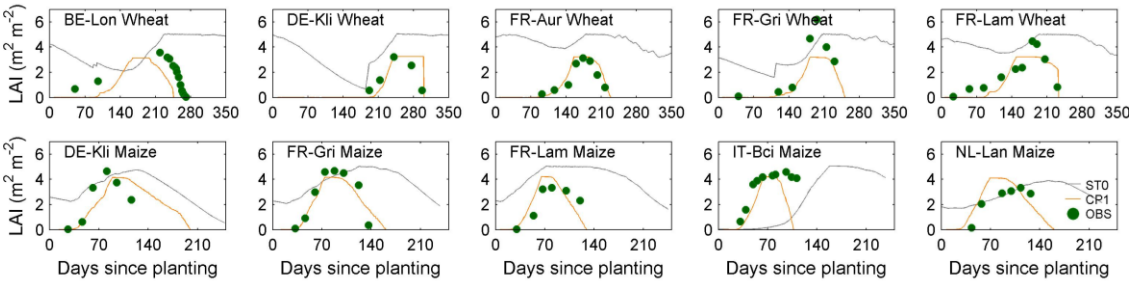
BE-Lon Wheat
DE-Kli Wheat
FR-Aur Wheat
FR-Gri Wheat
FR-Lam Wheat
DE-Kli Maize
FR-Gri Maize
FR-Lam Maize
IT-Bci Maize
NL-Lan Maize
LAI (m2 m-2)
Days since planting
ST0
CP1
OBS

1017

1018

1019

1020 Fig. 3

1021

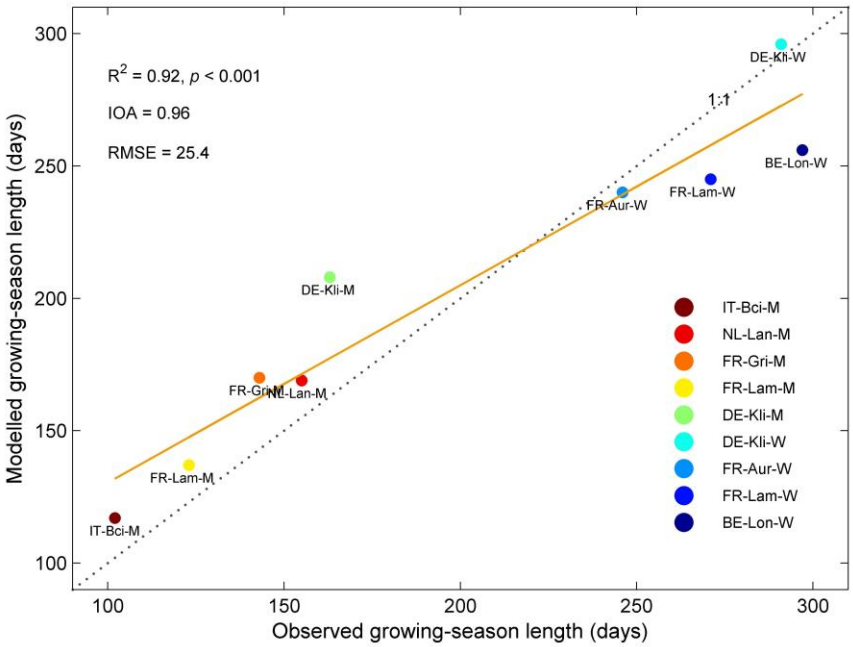

1022

1023

1024

1025

1026

1027 Fig. 4

1028

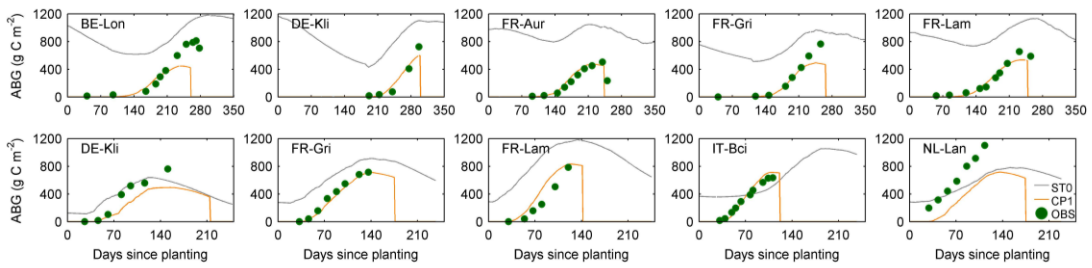

1029

1030

1031

1032

1033 Fig. 5

1034

1035

1036

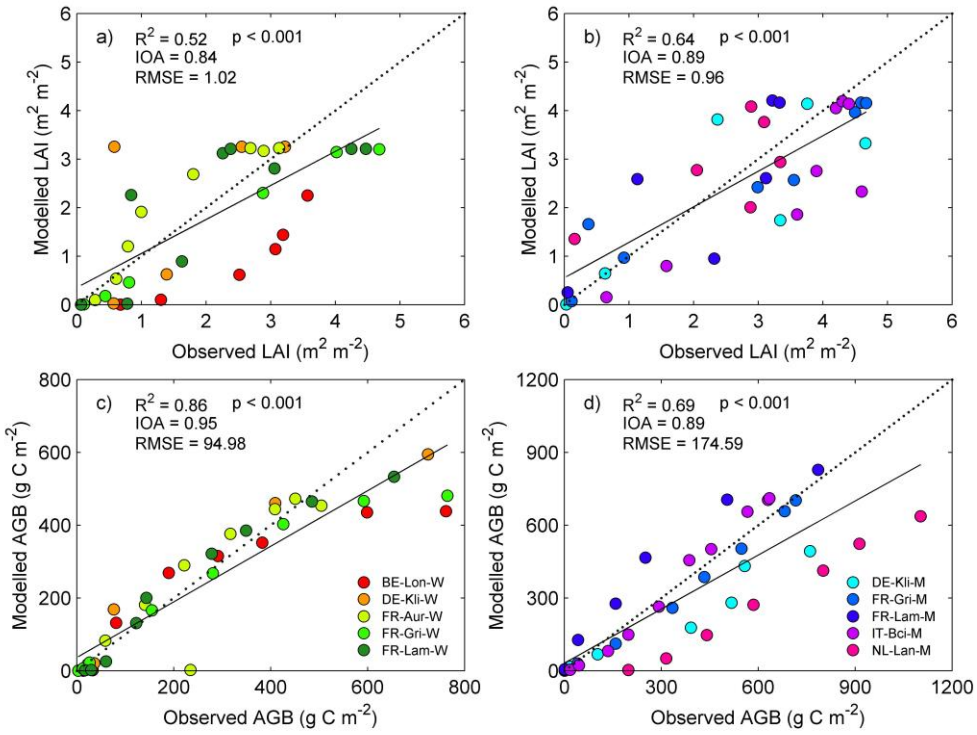

1037

1038

1039

1040

1041 Fig. 6

1042

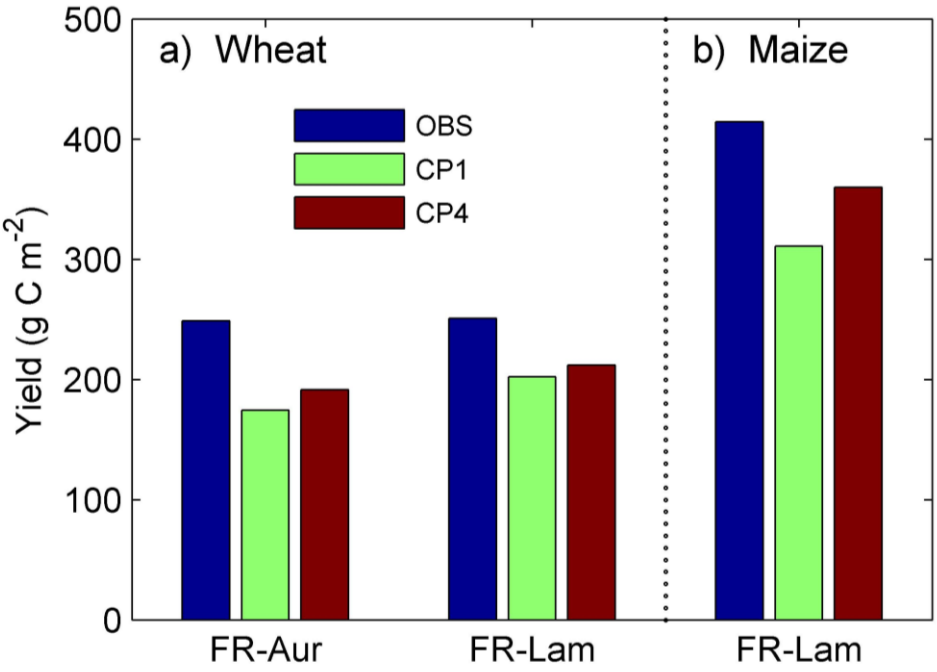

1043

1044

Fig. 7

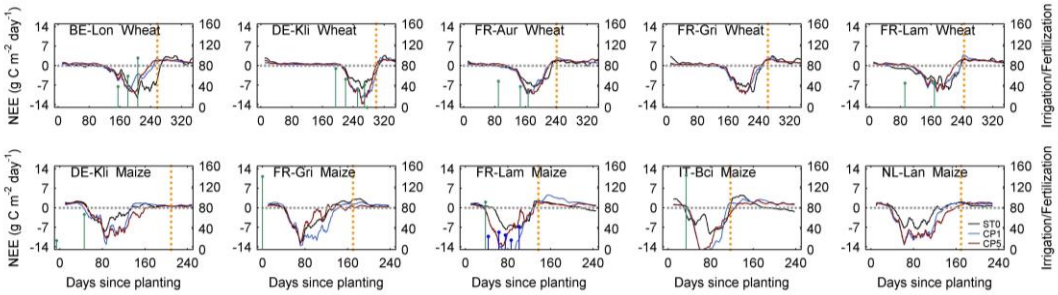
BE-Lon Wheat
DE-Kli Wheat
FR-Aur Wheat
FR-Gri Wheat
FR-Lam Wheat
DE-Kli Maize
FR-Gri Maize
FR-Lam Maize
IT-Bci Maize
NL-Lan Maize
NEE (g C m-2 day-1)
Irrigation/Fertilization
Days since planting
ST0
CP1
CP5

1052

1053

1054 Fig. 8

1055

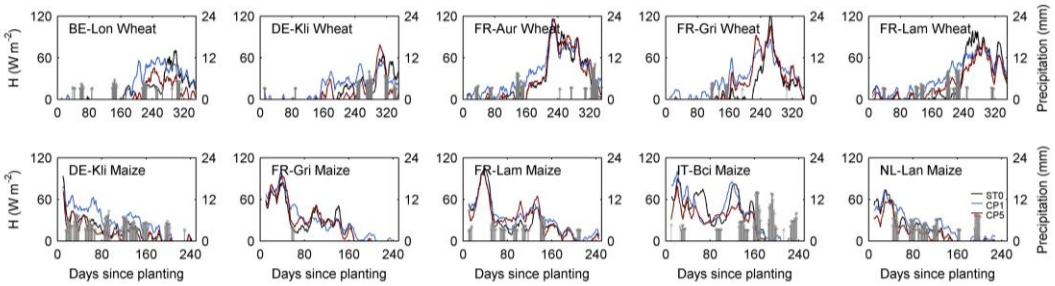

1056

1057

1058

Fig. 9

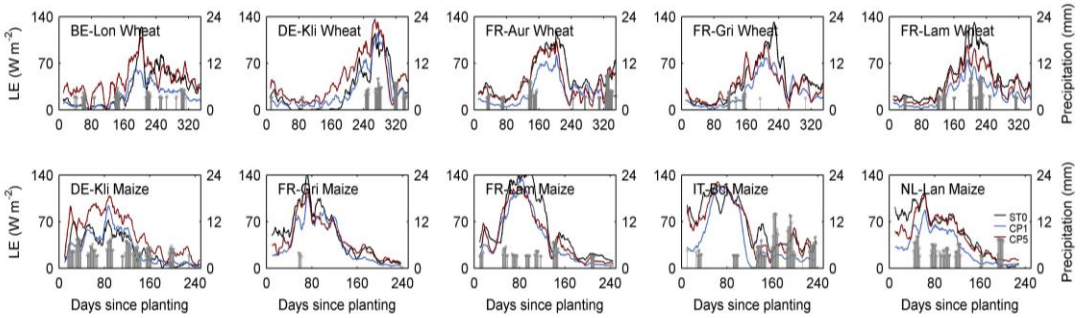
BE-Lon Wheat
DE-Kli Wheat
FR-Aur Wheat
FR-Gri Wheat
FR-Lam Wheat
DE-Kli Maize
FR-Gri Maize
FR-Lam Maize
IT-Bci Maize
NL-Lan Maize
LE (W m-2)
Precipitation (mm)
Days since planting
ST0
CP1
CP5

Figure 10.

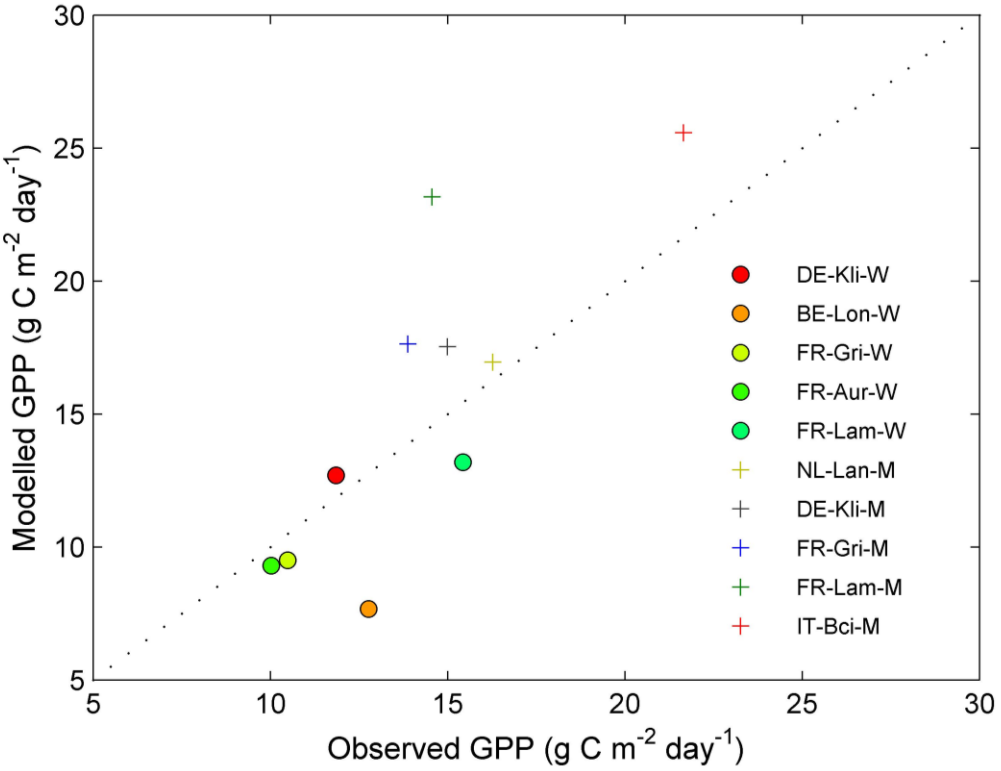
Modelled GPP (g C m-2 day-1)
Observed GPP (g C m-2 day-1)
5
10
15
20
25
30
DE-Kli-W
BE-Lon-W
FR-Gri-W
FR-Aur-W
FR-Lam-W
NL-Lan-M
DE-Kli-M
FR-Gri-M
FR-Lam-M
IT-Bci-M